Single-Channel Function of Recombinant Type 2 Inositol 1,4,5-Trisphosphate Receptor

Josefina Ramos-Franco, Dan Bare, Sean Caenepeel, Alma Nani, Michael Fill, and Gregory Mignery
Department of Physiology, Loyola University Chicago, Maywood, Illinois 60153 USA

ABSTRACT A full-length rat type 2 inositol 1,4,5-trisphosphate ($InsP_3$) receptor cDNA construct was generated and expressed in COS-1 cells. Targeting of the full-length recombinant type 2 receptor protein to the endoplasmic reticulum was confirmed by immunocytochemistry using isoform specific affinity-purified antibodies and $InsP_3$R-green fluorescent protein chimeras. The receptor protein was solubilized and incorporated into proteoliposomes for functional characterization. Single-channel recordings from proteoliposomes fused into planar lipid bilayers revealed that the recombinant protein formed $InsP_3$- and Ca^{2+}-sensitive ion channels. The unitary conductance (~250 pS; 220/20 mM Cs^+ as charge carrier), gating, $InsP_3$, and Ca^{2+} sensitivities were similar to those previously described for the native type 2 $InsP_3$R channel. However, the maximum open probability of the recombinant channel was slightly lower than that of its native counterpart. These data show that our full-length rat type 2 $InsP_3$R cDNA construct encodes a protein that forms an ion channel with functional attributes like those of the native type 2 $InsP_3$R channel. The possibility of measuring the function of single recombinant type 2 $InsP_3$R is a significant step toward the use of molecular tools to define the determinants of isoform-specific $InsP_3$R function and regulation.

INTRODUCTION

The inositol 1,4,5-trisphosphate receptor ($InsP_3$R) gene encodes an intracellular Ca^{2+} release channel that is fundamental to many intracellular Ca^{2+} signaling processes in metazoans. The $InsP_3$R channels, a family of three highly conserved isoforms, mobilize intracellular Ca^{2+} in response to $InsP_3$ generated by surface membrane receptor-activated hydrolysis of phosphatidyl-inositol 4,5 bisphosphate.

Despite the high degree of amino acid conservation between the three $InsP_3$R homologs, each isoform has a unique pattern of regulation by $InsP_3$ and cytosolic Ca^{2+}. The three $InsP_3$R proteins have different $InsP_3$-binding affinities. Type 2 $InsP_3$R has the highest affinity, and type 3 has the lowest (Südhof et al., 1991; Newton et al., 1994; Perez et al., 1997; Miyakawa et al., 1999). These isoform-specific differences in $InsP_3$ sensitivity were confirmed at the single-channel level after incorporation of isolated channels into artificial planar lipid bilayers (Watras et al., 1991; Perez et al., 1997; Ramos-Franco et al., 1998a; Hagar et al., 1998) and patch clamping of *Xenopus* oocyte nuclei (Mak et al., 1998). Single-channel studies also revealed that the native $InsP_3$R channels have isoform-specific differences in Ca^{2+} sensitivity. The Ca^{2+} sensitivity of the type 1 $InsP_3$R channel is bell-shaped (Bezprozvanny et al., 1991; Ramos-Franco et al., 1998a), suggesting that high cytosolic Ca^{2+} concentrations inhibit the channel. In contrast, the Ca^{2+} sensitivities of the native type 2 and type 3 channels are sigmoidal, implying that these channels are not regulated by the same intrinsic Ca^{2+}-dependent inhibition mechanism (Ramos-Franco et al., 1998a; Hagar et al., 1998). Thus single $InsP_3$R channel studies have generated valuable insights into $InsP_3$-dependent intracellular Ca^{2+} signaling, while also generating interesting new questions regarding isotype-specific $InsP_3$R function.

Kaftan et al. (1997) and Mak et al. (1998) suggest that $InsP_3$ modulates the Ca^{2+} sensitivity of the native type 1 channel. Kaftan et al. (1997) have proposed that two different types of $InsP_3$ binding sites (i.e., low and high affinity) modulate the Ca^{2+} sensitivity and consequently that $InsP_3$ levels define the biphasic nature of Ca^{2+} sensitivity for the type 1 channel. Mak et al. (1998) propose that $InsP_3$ acts solely at a single high-affinity site to "tune" the Ca^{2+} inhibition of $InsP_3$R channel. The type 2 and type 3 channels may lack such complex interactive Ca^{2+} and $InsP_3$ regulation (Ramos-Franco et al., 1998a; Hagar et al., 1998). The type-specific nature of Ca^{2+}-dependent inhibition may also involve the presence of an associated nonprotein factor (Watras et al., 1999). Presumably, this factor would be missing or does not associate with the native type 2 or type 3 channels. Furthermore, it has been suggested that certain closely associated regulatory proteins (e.g., FKBP12, calmodulin, calcineurin, etc.; Cameron et al., 1995; Michikawa et al., 1999) may also modulate $InsP_3$R channel function and thus may contribute to isoform-specific regulation. Studies utilizing recombinant $InsP_3$R channels can effectively be applied to test such proposals.

Although all three $InsP_3$R have been cloned, only the single-channel function of the recombinant type 1 $InsP_3$R has been well defined in planar lipid bilayers. Two groups independently confirmed that the full-length rat type 1 cDNA encodes channels with Ca^{2+} and $InsP_3$ sensitivity similar to that of the native type 1 $InsP_3$R channel (Kaznacheyeva et al., 1998; Ramos-Franco et al., 1998b). A

Received for publication 9 August 1999 and in final form 24 May 2000.

Address reprint requests to Dr. Gregory Mignery, Department of Physiology, Loyola University Chicago, 2160 South First Avenue, Maywood, IL 60153. Tel.: 708-216-1181; Fax: 708-216-5158; E-mail: gmigner@luc.edu.

0006-3495/00/09/1388/12 $2.00

full-length construct of the type 3 $InsP_3R$ exists but has not yet been evaluated in single-channel studies using planar lipid bilayers. Recently, however, the recombinant type 3 cRNA has been injected into *Xenopus* oocytes, and its single-channel properties were defined in patch-clamp studies (Mak et al., 2000). The first single-channel recordings of the recombinant type 2 $InsP_3R$ channels will thus be a significant step toward defining the mechanisms that underlie the functional heterogeneity of the three $InsP_3R$ channel isoforms. However, defining the single-channel function of the type 2 $InsP_3R$ channel will require the generation of an appropriate full-length cDNA construct.

The goal of this study was to construct, express, and functionally characterize a full-length rat type 2 $InsP_3R$ cDNA. A full-length type 2 expression plasmid was assembled from overlapping cDNAs (Mignery et al., 1990; Südhof et al., 1991) and expressed in COS-1 cells. The recombinant type 2 protein specifically bound $InsP_3$ and formed cationic ion channels when incorporated into planar lipid bilayers. The permeation properties and $InsP_3/Ca^{2+}$ regulation of the recombinant channels were similar to those of the native type 2 $InsP_3R$ channel. This type 2 $InsP_3R$ cDNA, therefore, represents a significant tool for future $InsP_3R$ structure-function studies and will provide the means to dissect the molecular determinants of the $InsP_3R$ functional diversity. A mutagenesis-based experimental strategy can now be applied to dissect the molecular aspects of the putative $InsP_3/Ca^{2+}$ regulatory interactions and assess contributions of certain titratable factors or regulatory proteins.

MATERIALS AND METHODS

Materials

[^{3}H]Inositol 1,4,5-trisphosphate (21 Ci/mmol) was obtained from NEN Life Science Products (Boston, MA). Unlabeled inositol 1,4,5-trisphosphate ($InsP_3$) was purchased from LC Laboratories (Woburn, MA), and heparin was from Sigma (St. Louis, MO). The lipids, phosphatidylserine, phosphatidylcholine, and phosphatidylethanolamine were obtained from Avanti Polar Lipids (Alabaster, AL).

Antibodies

The antibodies designated as T2NH and T2C used in this study recognize either the amino- or carboxyl-terminal regions of the type 2 $InsP_3R$ protein. The anti-peptide T2NH antibody is directed against the sequence CP-DYRDAQNEGKTVRDGELP (residues 320–338), and T2C recognizes the carboxyl-terminal 22 amino acids (CNKQRLGFLGSNTPHENH-HMPPH). These peptide antibodies were affinity purified using the immunogenic peptide. The secondary antibodies used in immunofluorescence studies were fluorescein isothiocyanate- and Texas Red-conjugated goat anti-rabbit IgG from ICN Pharmaceuticals (Aurora, OH). The type 1 carboxyl-terminal antibody used corresponds to amino acid residues 2731–2749 of the type 1 sequence and has been previously described in detail (Mignery et al., 1989; Ramos-Franco et al., 1998b).

Expression plasmid construction

The full-length type 2 $InsP_3R$ plasmid (p$InsP_3R$-T2) was assembled from overlapping cDNA clones originally isolated from a rat brain library (Südhof et al., 1991). Briefly, the ~1.9-kb *Bam*HI_{6631}/*Hin*$dIII_{8535}$ (subscripted numbers indicate nt positions in type 2 cDNA sequence, accession number X61677) fragment was excised from pI15, inserted into pBluescript to form plasmid A, cut with *Hin*dIII, Klenow DNA polymerase repaired, and religated (plasmid $B_{6631-8535}$). The *Bam*HI fragment of pI15 encompassing nt. 5830–6631 was inserted to generate plasmid $C_{5830-8535}$. Next the *Sma*I_{5927}/*Hin*$dIII_{6382}$ and *Eco*RI_{5616}/*Sma*I_{5927} from pI15 and pI41 (respectively) were inserted into pBluescript forming plasmid $D_{5616-6382}$. To this, a *Bam*HI_{3980}/*Nco*I_{4970} of pI65 and the *Nco*I_{4970}/*Eco*RI_{5616} from pI53 were inserted (plasmid $E_{3980-6382}$). The *Sac*I_{2268}/*Pst*I_{3475} of pI70 was ligated into a plasmid intermediate, and the *Pst*I fragment of pI70 (nt 3475–3904) was then inserted (plasmid $F_{2268-3904}$). The *Bgl*II_{3797}/*Eco*RI_{4700} fragment was ligated to this plasmid, generating plasmid $G_{2268-4700}$.

These plasmids were then used to assemble the full-length expression construct as follows. The *Bsm*I_{4490}/*Hin*$dIII_{6382}$ fragment of plasmid E was inserted into plasmid G, which was digested with *Bsm*I and *Hin*dIII (plasmid $H_{2268-6382}$). This plasmid (H) was digested with *Hin*dIII and *Xho*I, and the *Hin*$dIII_{6382}$/*Xho*I_{8535+V} of plasmid C was inserted, generating plasmid $I_{2268-8535}$. Next the *Eco*RI_1/*Kpn*I_{2440} of pIP_3R2-Stop1078 (Südhof et al., 1991) was ligated into similarly digested pCMV5 (plasmid J_{1-2440}). To this the *Kpn*I_{7260}/*Sal*$_{8535+V}$ of plasmid I was inserted, forming plasmid $K_{1-2440,\ 7260-8535}$. The final step involved the insertion of the *Kpn*I fragment of plasmid I (nt 2440–7260) and produced our full-length type 2 $InsP_3R$ expression plasmid, p$InsP_3R$-T2.

A type 2 $InsP_3R$ chimera amino-terminally tagged with enhanced green fluorescent protein (EGFP) (pEGFP-T2C573) was generated by inserting the *Bam*HI_{6632}/*Xba*I_{8535+V} fragment of the type 2 plasmid (p$InsP_3R$-T2) into similarly digested pEGFP-C1 (Clontech, Palo Alto, CA). This construct encodes EGFP fused to the carboxyl-terminal 573 residues of the type 2 receptor.

A full-length type 1 $InsP_3R$-green fluorescent protein chimera (pEGFP-T1FL) was constructed using a custom enhanced green and blue fluorescent protein vector in which the 1081 amino-terminal amino acids were inserted. This plasmid was digested with *Kpn*I and *Xba*I, removing nts 1589–3571 of the receptor and the enhanced blue fluorescent protein carboxyl-terminal tag. To this, the *Kpn*I-*Xba*I fragment (nts 1589–9465) of the type 1 $InsP_3R$ was inserted to generate the EGFP-full-length type 1 $InsP_3R$ chimera. Construction of the full-length type 1 $InsP_3R$ (p$InsP_3R$-T1) construct was previously described (Mignery et al., 1990).

COS cell transfections

COS-1 cells were transiently transfected either singly or doubly with the p$InsP_3R$-T1, p$InsP_3R$-T2, pEGFP-T1FL, pEGFP-T2C573 expression plasmids, using the diethylaminoethyl-dextran method as described by Gorman (1985). COS-1 cells mock transfected with sheared salmon sperm (SS) DNA served as the negative control. Cells were incubated at 37°C in 5% CO_2 for 48–72 h before harvesting for biochemical and functional analysis. Typical transfection efficiencies were 50% or greater, as determined by indirect immunofluorescence or via the EGFP reporter chimeras, although the efficiency of doubly transfected cells was less (~30%).

Immunocytochemical analysis

Transiently transfected COS cells were harvested by brief trypsinization followed by plating onto poly-D-lysine-coated glass coverslips. After an attachment interval, the cells were fixed with 4% paraformaldehyde in 200 mM phosphate buffer, permeabilized with 0.3% Triton X-100 in phosphate-buffered saline, and blocked in buffer containing 10% goat serum.

Expression of pInsP$_3$R-T2 and pInsP3R-T1 was detected by incubation with the affinity-purified anti-peptide antibodies T2NH, T2C, and T1C. Coverslips were then incubated with a fluorescein isothiocyanate-goat anti-rabbit secondary antibody. Cells expressing pEGFP-T2 and pEGFP-T1FL were fixed with 4% paraformaldehyde in 200 mM phosphate buffer, washed in phosphate-buffered saline, and imaged directly. COS-1 cells that were cotransfected with EGFP plasmids and either pInsP$_3$R-T2 or pInsP$_3$R-T1 were reacted with T2C or T1C, respectively, and counterstained with Texas Red–goat anti-rabbit secondary antibody. All coverslips were analyzed with a Nikon Diaphot 300 inverted microscope and imaged with a Diagnostics Spot-II digital camera and software.

Microsome preparation, solubilization, and gradient sedimentation

COS-1 cells transfected with pInsP$_3$-T2, pInsP$_3$R-T1, or SS DNA were harvested 48–72 h after transfection. Microsomes were prepared as described previously (Mignery et al., 1990). Briefly, COS-1 cells were washed with phosphate-buffered saline; harvested by scraping into 50 mM Tris-HCl (pH 8.3), 1 mM EDTA, 1 mM 2-mercaptoethanol, 1 mM phenylmethylsulfonyl fluoride (PMSF); and lysed by 40 passages through a 27-gauge needle. Membranes were pelleted by a 20-min centrifugation (289,000 $\times$ g_{av}), resuspended in buffer, and either used immediately or frozen at -80°C. Microsomal fractions were solubilized in 50 mM Tris-HCl (pH 8.3), 1 mM EDTA, 1 mM 2-mercaptoethanol, 1 mM PMSF, 1.8% 3-[(3-cholamidopropyl)dimethylammonio]-1-propane sulfonate (CHAPS) on ice for 1 h. Insoluble fractions were eliminated by a 10-min centrifugation at 289,000 $\times$ g_{av}, and the supernatants containing the solubilized receptor were fractionated through 5–20% sucrose (w/v) gradients as previously described (Mignery et al., 1989). Gradient fractions containing the InsP$_3$R protein were then identified by immunoblotting with the T2NH and T2C antibodies and reconstituted into proteoliposomes as previously described (Mignery et al., 1992; Perez et al., 1997; Ramos-Franco et al., 1998b).

[^{3}H]InsP$_3$ saturation binding

InsP$_3$ binding to membrane preparations from COS-1 cells transfected with pInsP$_3$R-T2 membrane preparations was performed in the presence of increasing concentrations of [^{3}H]InsP$_3$ ranging from 0.038 to 26.3 nM. Each assay contained 50 μg protein in binding buffer (50 mM Tris-HCl, 1 mM EDTA, 1 mM β-mercaptoethanol, pH 8.3) and was conducted like the centrifugation binding assay previously described (Mignery et al., 1990). The binding assays were incubated on ice for 10 min in the presence of [^{3}H]InsP$_3$, and then microsomes were pelleted with a 10-min 289,000 $\times$ g_{av} centrifugation. The supernatants were removed from the assay tube, and the membrane pellet was solubilized in 1% sodium dodecyl sulfate (SDS) and counted in a Beckman liquid scintillation counter. All assays were performed in quadruplicate, and nonspecific [^{3}H]InsP$_3$ binding for each concentration was determined in the presence of 30 μM unlabeled InsP$_3$. Similar results were obtained from two independent assays.

[^{3}H]InsP$_3$ competition binding

Displacement-competition assays of [^{3}H] InsP$_3$ binding in the presence of increasing concentrations of unlabeled InsP$_3$ were performed on microsomal fractions from COS-1 cells transfected with either pInsP$_3$R-T2 or -T1 expression vectors. Each 100-μl assay contained 50 μg protein in binding buffer (above). Quadruplicate assays were incubated on ice for 10 min in the presence of [^{3}H]InsP$_3$ (3.14 nM) and increasing concentrations (0–20 μM) of unlabeled InsP$_3$ competitor and then pelleted with a 10-min 289,000 $\times$ g_{av} centrifugation. Nonspecific binding for each sample set was determined in the presence of 30 μM unlabeled InsP$_3$. Binding was determined by scintillation counting, and data were analyzed using Graph Pad Prism v3.0. Similar results were obtained from two independent assays.

Immunoprecipitations

Transfected COS-1 cells were harvested and microsomes were prepared as described above. Microsomes were solubilized with mixing on ice for 2 h in buffer A (1% CHAPS, 150 mM sodium chloride, 10 mM Tris-HCl (pH 7.4), 1 mM EDTA, 1 mM EGTA, 1 mM PMSF, and 2% bovine serum albumin). Samples were clarified by centrifugation at 106,120 $\times$ g_{av} for 5 min at 4°C. The supernatants were removed and mixed with 2 μl ($\sim$ 2 μg, 1:250 dilution) of the immunoprecipitating antibody (T2NH) directed against the amino terminus of the type 2 InsP$_3$R. The samples were incubated on ice for 4 h. Samples were clarified by centrifugation in a microcentrifuge (16,000 $\times$ g_{av}) at 4°C for 5 min, and the supernatants were retained. To each supernatant fraction, 20 μl of a 10% protein A-Sepharose CL4B (Pharmacia) slurry was added and incubated at 4°C for 2 h with gentle agitation. The antigen-IgG-protein A-Sepharose conjugates were pelleted by a 10-s centrifugation at 16,000 $\times$ g_{av}. The samples were washed three times for 5 min each in 0.5 ml buffer B (1% Triton X-100, 150 mM sodium chloride, 10 mM Tris-HCl (pH 7.4), 1 mM EDTA, 1 mM EGTA, and 1 mM PMSF), two times in buffer C (1% Triton X-100, 300 mM sodium chloride, 10 mM Tris-HCl (pH 7.4), 1 mM EDTA, 1 mM EGTA, and 1 mM PMSF), and once briefly in buffer D (10 mM Tris-HCl (pH 7.4), 1 mM EDTA, 1 mM EGTA, 1 mM PMSF). Bound antigen was released from the protein A beads by the addition of sodium dodecyl sulfate-polyacrylamide gel electrophoresis (SDS-PAGE)-sample buffer and boiling for 3 min.

SDS-PAGE and immunoblotting

COS-1 cell microsomes and sucrose gradient fractions were analyzed by 5% SDS-PAGE as described previously (Mignery et al., 1990). This was followed by immunoblotting and detection using chemiluminescence reagents (Enhanced ECL; Amersham Life Sciences, Arlington Heights, IL).

Single-channel recording

Planar lipid bilayers were formed across a 220-μm-diameter aperture in the wall of a Delrin partition as described (Perez et al., 1997). Lipid bilayer-forming solution contained a 7:3 mixture of phosphatidylethanolamine and phosphatidylcholine dissolved in decane (50 mg/ml). Proteoliposomes were added to the solution on one side of the bilayer (defined as the *cis* chamber). The other side was defined as the *trans* chamber (virtual ground). Standard solutions contained 220 mM $CsCH_3SO_3$ *cis* (20 mM *trans*), 20 mM HEPES (pH 7.4), and 1 mM EGTA ($[Ca^{2+}]_{FREE}$ = 250 nM). Proteoliposome fusion was detected by a sudden increase in baseline leak current. Single InsP$_3$R opening events were observed on top of this baseline leak. The calcium salt used was either $CaCH_3SO_3$ or $CaCl_2$. The $[Ca^{2+}]_{FREE}$ was verified using a Ca^{2+} electrode. The Ca^{2+} electrodes employed the Ca-ligand ETH 129 in a polyvinyl chloride membrane at the end of a small (2 mm) polyethylene tube. These Ca^{2+} minielectrodes were made and used as described previously (Baudet et al., 1994). A custom current-voltage conversion amplifier was used to optimize single-channel recording. Acquisition software (pClamp; Axon Instruments, Foster City, CA), an IBM-compatible 486 computer, and a 12-bit A/D-D/A converter (Axon Instruments) were used. Single-channel data were digitized at 2 kHz and filtered at 1 kHz. Channel sidedness was determined by InsP$_3$ sensitivity. The orientation of the channels studied was such that the InsP$_3$-sensitive side (i.e., cytoplasmic side) was in the *cis* compartment.

RESULTS

Expression of type 2 $InsP_3R$

The $InsP_3R$ expression plasmid ($pInsP_3R$-T2) was assembled from overlapping cDNA clones (Südhof et al., 1991) and transiently transfected into COS-1 cells (Gorman, 1985). The full-length type 1 $InsP_3R$ expression plasmid ($pInsP_3R$-T1) and SS DNA were also transfected into COS-1 cells for comparison. The expression plasmids were under the control of the cytomegalovirus promoter (Mignery et al., 1990) and expressed high levels of immunoreactive protein, shown by Western blotting with the antibodies directed against the type 2 and type 1 receptor isoforms (Fig. 1). Equivalent amounts of microsomal protein (20 μg) from COS-1 cells transfected with $pInsP_3R$-T2, $pInsP_3R$-T1, or SS DNA were immunoblotted with the T2NH, T2C, and T1C antibodies (Fig. 1, *A–C*). These data reveal a prominent immunoreactive ~260-kDa protein, indicating that significant levels of the full-length type 2 protein were expressed (Fig. 1, *A* and *B*). Neither of the two type 2 antibodies (T2NH and T2C) reacted to a significant extent with the type 1 $InsP_3R$ expression product. A smaller immunoreactive band is observed in the $pInsP_3R$-T2 expression products with the use of T2NH antibody (Fig. 1 *A*). This band likely represents proteolysis of the full-length expression product or possibly premature translational termination. It does not appear to represent cross-reactivity with another protein species, because of the lack of signal in the adjacent SS DNA and $pInsP_3R$-T1 control lanes. An antibody that specifically recognizes the carboxyl-terminal end of the type 1 $InsP_3R$ protein (T1C) detected the type 1 $InsP_3R$ expression products (Fig. 1 *C*). The mock transfected (SS DNA) COS-1 cells had little detectable endogenous $InsP_3R$ signal (Fig. 1, *A–C*). The T1C antibody detected no type 1 $InsP_3R$ signal above that of the SS DNA control in cells expressing $pInsP_3R$-T2 expression products (Fig. 1 *C*). This indicates that overexpression of the type 2 $InsP_3R$ did not result in enhanced expression of endogenous type 1 $InsP_3R$. Previous studies have demonstrated similar results for the three endogenous isoforms in COS-1 cells overexpressing type 1 $InsP_3R$ splice variants (Ramos-Franco et al. 1998b).

Protein expression was also confirmed by using the T2NH antibody to immunoprecipitate the type 2 protein from CHAPS-solubilized microsomes of COS-1 cells transfected with either $pInsP_3R$-T2 or SS DNA (Fig. 1 *D*). No signal was observed in the control (SS DNA) sample, using T2C as the detection antibody. The smaller immunoreactive band with greater apparent mobility than the full-length receptor observed in the $pInsP_3R$-T2 expression products with the use of the T2NH antibody (Fig. 1 *A*) was not observed in the Western blot of immunoprecipitation products or in the immunoblot of expression products with the use of T2C. Similar results were obtained when T2C was used as the immunoprecipitating antibody, followed by immunodetection with T2NH antibody (data not shown).

$InsP_3$-binding properties

Equilibrium $InsP_3$ binding assays were performed using microsomal fractions from COS-1 cells transfected with $pInsP_3R$-T2 and SS DNA. The full-length type 2 recombinant $InsP_3R$ protein bound significant amounts of $InsP_3$, whereas the SS DNA control microsomes did not bind $InsP_3$ at significant levels above nonspecific background. These results are consistent with previous studies in which micro-

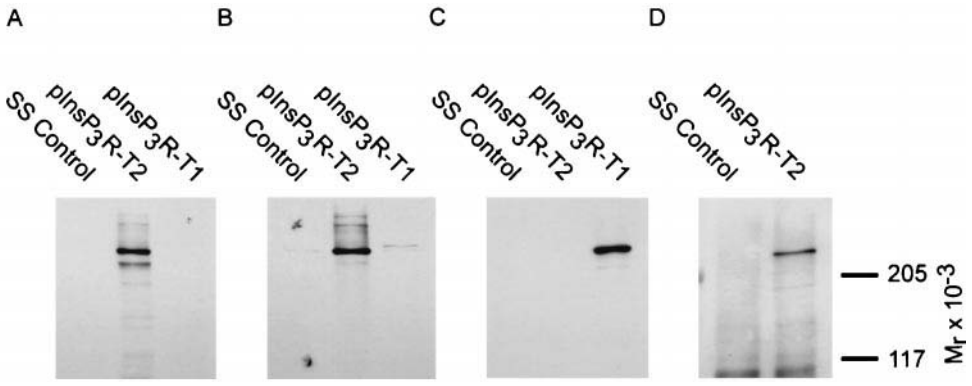

FIGURE 1 Analysis of type 2 $InsP_3R$ expression in transfected COS-1 cells by Western immunoblotting and immunoprecipitation. Microsomal protein (20 μg) isolated from COS-1 cells transiently transfected with salmon sperm DNA (SS control), rat type 2 $InsP_3R$ ($pInsP_3R$-T2), and rat type 1 $InsP_3R$ ($pInsP_3R$-T1) were resolved on 5% SDS-PAGE, transferred to nitrocellulose membranes, and immunoblotted. Western blots were reacted with (*A*) type 2 $InsP_3R$ amino-terminal (T2NH), (*B*) type 2 carboxyl-terminal (T2C), and (*C*) type 1 carboxyl-terminal (T1C) antibodies. (*D*) Microsomal proteins from COS-1 cells transfected with either salmon sperm DNA (SS control) or $pInsP_3R$-T2 were solubilized in CHAPS detergent and subjected to immunoprecipitation using the type 2 amino-terminal antibody (T2NH). Immunoprecipitable products were resolved on 5% SDS-PAGE and Western blotted using the type 2 specific carboxyl-terminal antibody. Note that no detectable signal is observed in the SS control, whereas there is a prominent immunoprecipitation product from COS-1 cells expressing $pInsP_3R$-T2.

somes of transfected COS-1 cells contained abundant amounts of immunoreactive receptor protein and bound significant amounts of [^{3}H]InsP_3 (Mignery et al., 1990; Südhof et al., 1991; Ramos-Franco et al., 1998b). Saturation binding assays were performed to determine the apparent affinity of the pInsP_3R-T2 expression product (Fig. 2 *A*). In these assays increasing amounts of radioligand were incubated with a constant amount of microsomal protein (50 μg) from transiently transfected COS-1 cells. Nonspecific binding was determined in all conditions with the use of 30 μM unlabeled InsP_3. Nonlinear regression analysis predicted an apparent K_d and a B_{max} of 16.9 nM and 0.29 pmol/mg protein, respectively (SE: K_d = 3.923 nM, B_{max} = 0.037 pmol/mg).

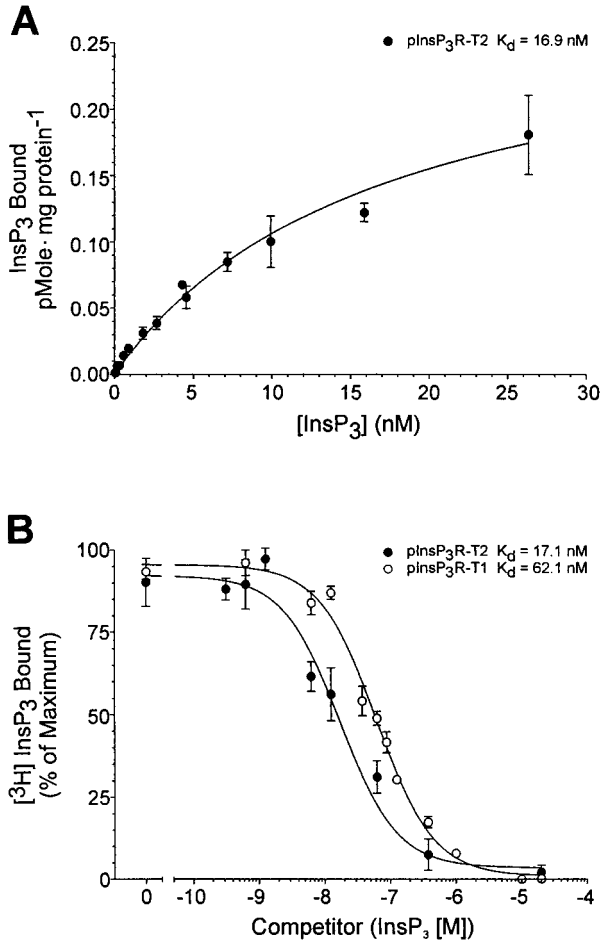

FIGURE 2 [^{3}H]InsP_3 binding to recombinant type 2 InsP_3R. (*A*) Saturation InsP_3 binding properties of microsomes from COS-1 cells transiently transfected with the full-length type 2 InsP_3R (pInsP_3R-T2). [^{3}H]InsP_3 concentrations ranged from 0.04 to 26.3 nM, and nonspecific binding was determined in the presence of 30 μM unlabeled InsP_3. (*B*) Comparison of recombinant type 1 and type 2 InsP_3R ligand-binding properties by competition binding. Microsomes from transiently transfected COS-1 cells expressing the full-length type 2 (pInsP_3R-T2) or the type 1 (pInsP_3R-T1) isoforms were incubated with 3.14 nM [^{3}H]InsP_3 and increasing concentrations of unlabeled InsP_3 competitor (0–20 μM).

Previously, Südhof and co-workers reported that the apparent affinities of the recombinant type 1 and type 2 InsP_3R isoform ligand-binding domain regions (NH_2-amino acids 1081 and 1078, respectively) differed by approximately threefold (Südhof et al., 1991). In those experiments, the type 2 ligand-binding domain exhibited the highest apparent affinity, with a predicted K_d of 27 nM, whereas the type 1 isoform had a K_d of 89 nM. To determine whether the recombinant full-length type 1 and type 2 isoforms exhibited similar heterogeneity in InsP_3 affinity, we performed InsP_3 competition binding assays (Fig. 2 *B*). Microsomes from COS-1 cells that were transfected with either pInsP_3R-T1 or pInsP_3R-T2 were incubated in the presence of a constant amount of [^{3}H]InsP_3 (3.14 nM) and increasing concentrations of unlabeled InsP_3 (0–20 μM) (Fig. 2 *B*). Nonspecific binding for each condition was determined using 30 μM unlabeled InsP_3. Nonlinear data analysis predicted K_d values of 17.1 and 62.1 nM for the full-length recombinant type 2 and type 1 receptor isoforms, respectively. This three- to fourfold difference is similar to that previously reported for the soluble ligand-binding regions (Südhof et al., 1991).

Immunolocalization

The expression and targeting of the type 2 recombinant InsP_3R protein in transfected COS-1 cells were analyzed by immunofluorescence microscopy, using the T1C, T2NH, and T2C antibodies and green fluorescent protein/type 1 and type 2 InsP_3R chimeras (Fig. 3). The type 1 InsP_3R has previously been shown to target to the endoplasmic reticulum (ER) and associated structures as a multipass integral membrane protein in transfected COS-1 cells and is included as a localization standard (Takei et al., 1994; Ramos-Franco et al., 1998b; Galvan et al., 1999). COS-1 cells overexpressing the full-length type 1 receptor (pInsP_3R-T1) were labeled with T1C antibody (Fig. 3 *1*). The expressed protein is localized to tubular membranous networks that are widespread throughout the cell and have morphological characteristics of the endoplasmic reticulum. Previous studies demonstrated that this reticular network was immunoreactive for the ER marker Bip (Takei et al., 1994). COS-1 cells transfected with pInsP_3R-T2 reveal numerous brightly immunoreactive cells with antibodies T2NH and T2C (Fig. 3, *2* and *3*). The expressed full-length type 2 InsP_3R was targeted to reticular networks throughout the cell and the tips of extending processes. This targeting was indistinguishable from that observed with the type 1 receptor. Some perinuclear enrichment was evident with both the type 1- and type 2-expressing cells. The intense perinuclear signal is due to saturation of the digital acquisition exposure intervals necessary to visualize the fine reticular meshwork in the cell periphery. Nontransfected COS-1 cells visible within the fields or those transfected with control SS DNA

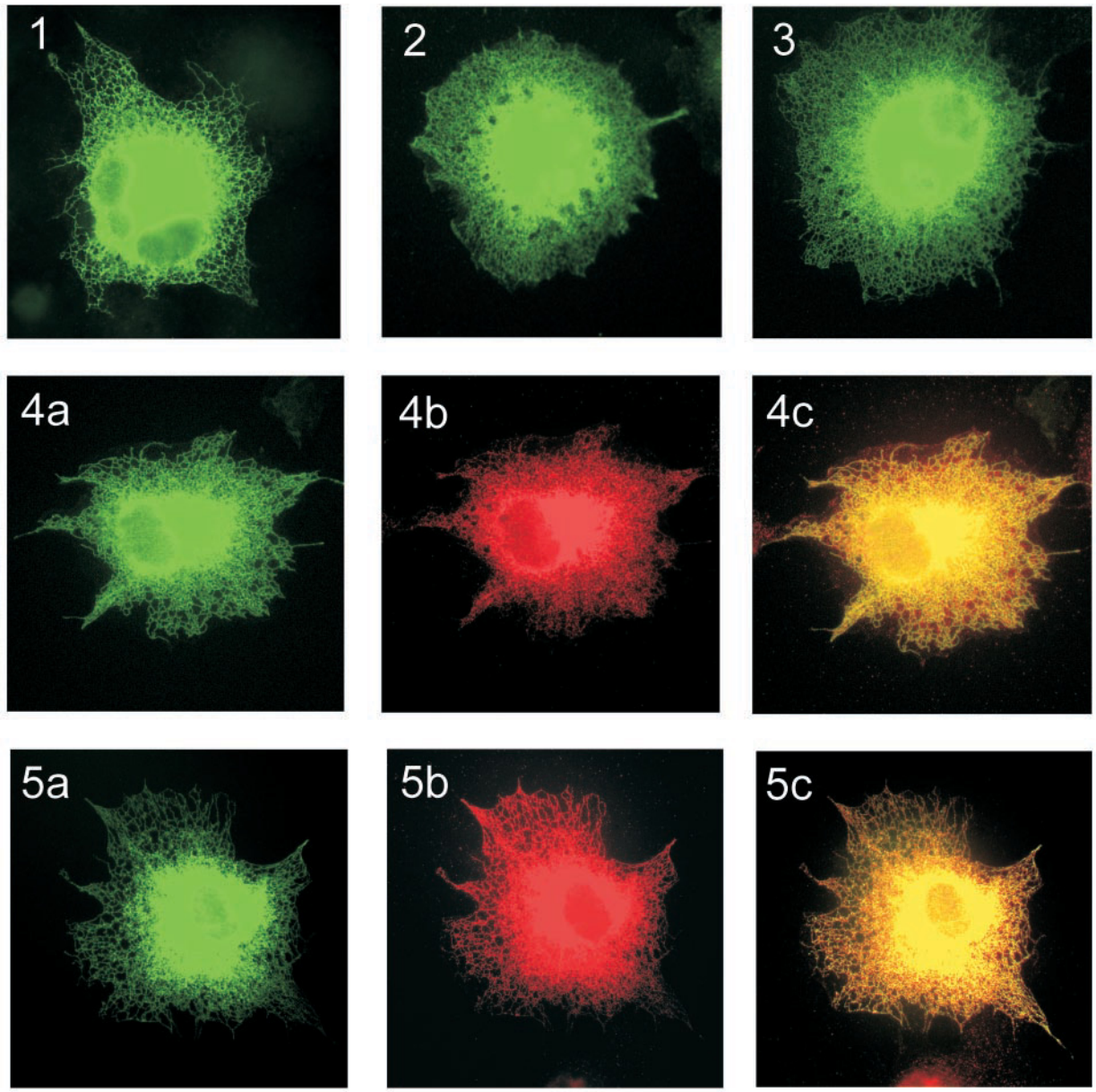

FIGURE 3 Targeting and localization of the type 2 $InsP_3R$. COS-1 cells were singly transfected or cotransfected with type 1 and type 2 $InsP_3R$ expression plasmids and were analyzed by immunofluorescence microscopy. (*1*) Type 1 $InsP_3R$-positive control: COS-1 cell expressing full-length type 1 receptor ($pInsP_3R$-T1) that was immunolabeled using the type 1 carboxyl-terminal antibody (T1C). Note the clear reticular localization in the cell periphery. (*2* and *3*) Expression of full-length type 2 $InsP_3R$: COS-1 cells transfected with the full-length type 2 expression plasmid ($pInsP_3R$-T2) and detected with the type 2-specific amino-terminal antibody (T2NH) (*2*) or the carboxyl-terminal antibody (T2C) (*3*). (*4a–c*) COS-1 cells cotransfected with a GFP-tagged full-length type 1 (pEGFP-T1FL) and the full-length type 2 ($pInsP_3R$-T2) $InsP_3R$ vectors. GFP-type 1 $InsP_3R$ (pEGFP-T1FL) expression is illustrated in *4a*, and type 2 ($pInsP_3R$-T2) expression identified using T2C antibody is shown in *4b*. The overlapping distribution of both receptor isoforms as observed with simultaneous excitation of both the red and green wavelengths is pictured in *4c*. (*5a–c*) COS-1 cells cotransfected with a GFP-tagged type 2 construct containing the carboxyl-terminal 573 amino acids (pEGFP-T2C573) and the full-length type 1 $InsP_3R$ vectors ($pInsP_3R$-T1). GFP type 2 $InsP_3R$ expression is shown in *5a*, and type 1 expression identified using T1C antibody is shown in *5b*. *5c* shows the overlapping distribution of both receptor isoforms observed with simultaneous excitation of both the red and green wavelengths.

(not shown) exhibited little (if any) specific immunoreactivity to the T1C, T2NH, or T2C antibodies.

To further demonstrate that the type 1 and type 2 $InsP_3R$ proteins are targeted to the same membranous structures, COS-1 cells were cotransfected with type 1 and type 2 expression plasmids. To accomplish this we prepared a full-length type 1 $InsP_3R$ construct that was amino-terminally tagged with green fluorescent protein (GFP) (pEGFP-T1FL) and a type 2 $InsP_3R$ chimera (pEGFP-T2C573). The pEGFP-T2C573 chimera includes the carboxyl-terminal

573 amino acids, encompassing all of the membrane-spanning regions in the channel domain. Similar truncated type 1 expression plasmids have been shown to oligomerize and target as their full-length counterpart (Sayers et al., 1997; Kiselyov et al., 1999; Galvan and Mignery, unpublished observations). These chimeras were cotransfected with the full-length type 1 and type 2 $InsP_3R$'s (p$InsP_3R$-T1 and p$InsP_3R$-T2). COS-1 cells cotransfected with pEGFP-T1FL and p$InsP_3R$-T2 are illustrated in Fig. 3, *4a–c*. The pEGFP-T1FL expression products localize to the ER (Fig. 3 *4a*) and are indistinguishable from those of immunostained cells transfected with p$InsP_3R$-T1 (Fig. 3 *1*). Immunolabeling the cells with T2C and Texas Red secondary antibody revealed robust expression of the type 2 receptor (Fig. 3 *4b*) that was localized to the ER. Imaging the cell with a dual excitation filter set (Fig. 3 *4c*) reveals that the two recombinant proteins are located in the same structures. In the reciprocal experiment, COS-1 cells were cotransfected with p$InsP_3R$-T1 and pEGFP-T2C573 (Fig. 3, *5a–c*). The targeting of the type 2-GFP chimera (pEGFP-T2C573) expression product is shown in Fig. 3 *5a* and is identical to that observed for the full-length type 2 expression product with either T2NH or T2C antibodies (Fig. 3, *2* and *3*). The full-length type 1 receptor was visualized using T1C and Texas Red antibody (Fig. 3 *5b*), and the two expression products appear to colocalize when imaged with dual-wavelength filter sets (Fig. 3 *5c*). These results indicate that in COS-1 cells the recombinant type 1 and type 2 $InsP_3R$ isoforms target to the endoplasmic reticulum.

Properties of single recombinant type 2 $InsP_3R$ channel

The recombinant type 2 $InsP_3R$ protein expressed in transfected COS-1 cells was solubilized with CHAPS and enriched by sucrose density centrifugation on 5–20% linear gradients. The preparative gradients were fractionated and Western blotted, using T2NH and T2C antibodies to identify the recombinant receptor (Fig. 4). Note that the smaller immunoreactive band was observed in the Western blots of expressed proteins using T2NH (Fig. 1 *A*) sediments as an apparent monomer and was not found at significant levels in the fractions containing tetrameric type 2 $InsP_3R$ (e.g., fractions 14–18). This sedimentation profile (monomeric) is consistent for a receptor protein missing the carboxyl-terminal region (Mignery and Südhof, 1993; Galvan et al., 1999). Gradient fractions containing the enriched receptor (fractions 14–18) were reconstituted into liposomes as previously described (Perez et al., 1997; Ramos-Franco et al., 1998a,b). These $InsP_3R$-enriched proteoliposomes were then fused into artificial planar lipid bilayers. This strategy was previously applied by our laboratories to define the single-channel function of the native type 1, recombinant type 1, and native type 2 $InsP_3R$ Ca^{2+} channels (Perez et al., 1997; Ramos-Franco et al., 1998a,b). Here single-channel

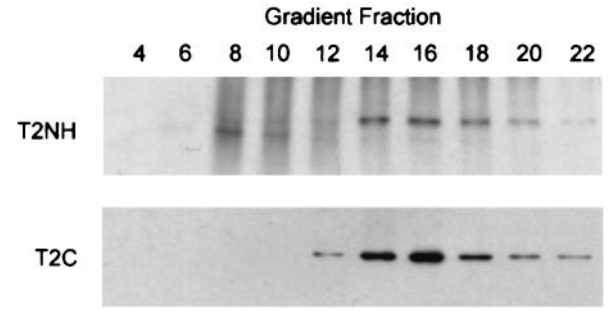

FIGURE 4 Partial purification of $InsP_3R$ proteins by sedimentation over sucrose density gradients. Microsomes from COS-1 cells transiently transfected with p$InsP_3R$-T2 were solubilized in 1.8% CHAPS and sedimented over 5–20% (w/v) sucrose gradients. An equivalent sample volume from each gradient fraction was analyzed by SDS-PAGE and immunoblotted with T2NH and T2C antibodies. Strong immunoreactive signals were detected in gradient fractions consistent with the sedimentation properties of $InsP_3R$ tetramers. Fractions containing the highest amounts of receptor (nos. 14–18) were used in the preparation of proteoliposomes for single-channel studies. Note that the smaller band observed using T2NH antibody (see also Fig. 1), which is hypothesized to represent a carboxyl-terminal proteolysis product or translational truncation, does not sediment with the bulk of the receptor and is most abundant in fraction 8. Sedimentation to this gradient position is typical for that of monomeric $InsP_3R$ protein (Galvan et al., 1999). (Fraction numbering starts at the top (5% sucrose) of the gradient.)

studies of the recombinant type 2 $InsP_3R$ channel were performed with similar solutions and experimental conditions. Thus the properties of the recombinant type 2 $InsP_3R$ and the properties of these other channels could be directly compared, providing a stronger context in which the data can be interpreted.

Functional attributes of single recombinant type 2 $InsP_3R$ were studied, using Cs^+ as the cationic charge carrier. The single-channel recording solutions contained 220 mM $CsCH_3SO_3$ *cis* (20 mM *trans*), 20 mM HEPES (pH 7.4), 1 mM EGTA, and 0.781 mM $CaCl_2$ ($[Ca^{2+}]_{FREE}$ = 250 nM). The $[Ca^{2+}]_{FREE}$ was verified using a Ca^{2+} electrode. In the absence of added $InsP_3$ the channel was quiescent, with only very rare opening events. The addition of 1 μM $InsP_3$ (*cis*) resulted in a channel that was spontaneously active, exhibiting frequent and rapid opening events (Fig. 5). The presence of 10 μM ryanodine had no effect on channel gating or permeation. No detectable $InsP_3$-sensitive, Cs^+-conducting channels were incorporated into the bilayer after fusion of proteoliposomes containing gradient fractions from control (SS DNA) transfected COS-1 cells. The absence of channels in the SS DNA control proteoliposomes demonstrates the low abundance of the endogenous receptors compared to liposomes containing the expressed recombinant protein. The ratio of the number of incorporation attempts to the number of type 2 channels observed was close to 5 (Table 1). This value is similar to that we previously described for the recombinant type 1 channels (Ramos-Franco et al., 1998b).

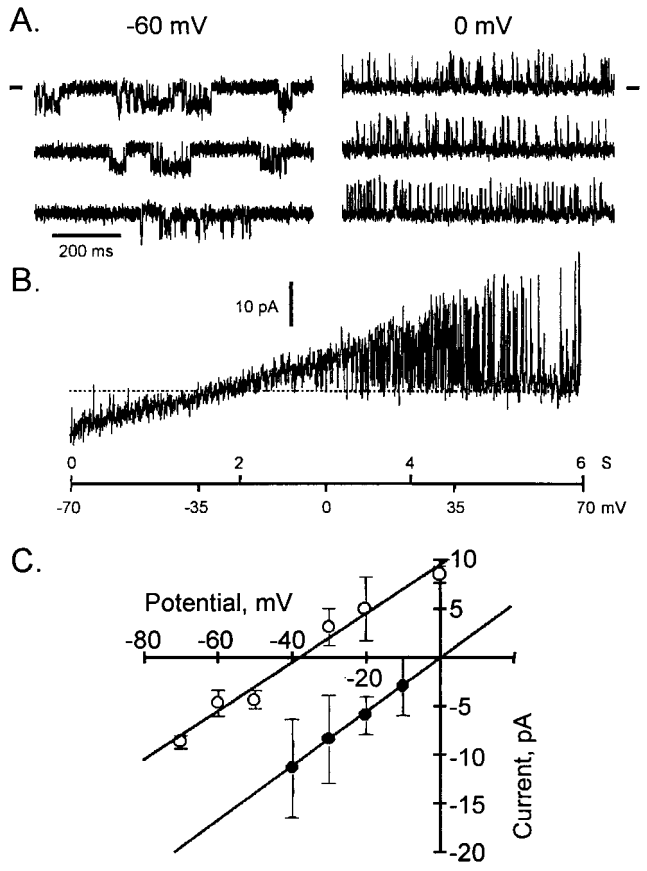

FIGURE 5 Sample recombinant type 2 $InsP_3R$ single-channel recordings. Single $InsP_3R$ channels were incorporated into planar lipid bilayers by fusion of proteoliposomes. Recording solutions contained 20 mM HEPES (pH 7.4), 1 mM EGTA (250 nM free Ca), and 1 μM $InsP_3$. (*A*) Single-channel recordings at two different steady-state membrane potentials (−60 and 0 mV). Open events are shown as downward deflections at −60 mV and upward deflections at 0 mV. The zero-current level is marked. Records are characterized by frequent fast opening events. (*B*) Single-channel recording during a voltage ramp. Open events at positive potentials are upward deflections from the marked zero-current level (*dotted line*). Leak current was subtracted. (*C*) Unitary current-voltage relationship. Points represent means and standard errors of many measurements from several single $InsP_3R$ channels (n = 5–8). Open symbols indicate measurement in a 220/20 mM Cs^+ gradient. The slope conductance was 249 ± 12 pS with a reversal potential of −38 mV. Filled symbols indicate measurement in symmetrical 220 mM Cs^+. The slope conductance was 276 ± 8 pS with a reversal potential of 0 mV.

Sample single-channel recordings at two different steady-state membrane potentials are presented in Fig. 5 *A*. Open events at −60 mV are shown as downward deflections from the marked zero-current level. The amplitude of the unitary current at −60 mV was near −5 pA. Open events at 0 mV are shown as upward deflections from the zero-current level. Unitary current amplitude at this potential was near 8 pA. Unitary current was recorded during slow membrane potential ramps (−70 to +70 mV; Fig. 5 *B*). The data in Fig. 5 *B* were collected while the voltage was slowly ramping at a relatively slow sample rate (0.5 kHz). The reversal potential was −32 mV, indicating a cationic channel. These data illustrate the relatively high inherent variability in stationary open probability and open times between different individual $InsP_3R$ channels.

TABLE 1 Frequency of $InsP_3R$ channel incorporation into planar lipid bilayers

Preparation	No. of attempts	No. of incorporations	Success rate
p$InsP_3R$-T2	158	31	20%
SS control	281	0	0

Unitary current was measured at several steady-state membrane potentials, plotted, and fit by a linear regression (Fig. 5 *C*). The slope of the unitary current-voltage relationship was 249 ± 12 pS, and the reversal potential was −38 mV. The negative reversal potential here also indicates that the channel is selective for the permeable cation. There was no clear rectification of the current-voltage plot in these asymmetrical solutions (220/20 Cs^+). Three factors may contribute to this observation. First, The K_d for Cs^+ in the $InsP_3R$ pore may be close to 20 mM. Second, net currents were not measured far from the reversal potential. Third, the inherent error level associated with measuring small net currents may make subtle differences difficult to detect. For clarity, the unitary current-voltage relationship in symmetrical salt solutions (220/220 $CsCH_3SO_3$) is also shown (Fig. 5 *C*).

The $InsP_3$ sensitivity of the recombinant type 2 $InsP_3R$ channel was defined. Sample single-channel recordings at two different $InsP_3$ concentrations are presented in Fig. 6 *A*. These recordings were made at 0 mV, and open events are shown as upward deflections. The current carrier was a monovalent cation (Cs^+; 220/20 mM $CsCH_3SO_3$ gradient) to avoid free Ca^{2+} concentration changes in the channel's microenvironment. The free Ca^{2+} concentration was buffered (1 mM EGTA) at 250 nM on both sides of the channel. The $InsP_3$ was added only to the cytoplasmic side of the channel (*cis* side). As stated above, P_o and open time vary with time and vary between different individual $InsP_3R$ single channels (compare Figs. 6 *A* and 5 *A*). Thus the average open probability (P_o) of the channel over several minutes is plotted as a function of $InsP_3$ concentration in Fig. 6 *B*. These data represent recordings from four different channels. The dose of $InsP_3$ required for half-maximum activation (EC_{50}) of the recombinant type 2 $InsP_3R$ channel (*solid line*, R-T2) was 122 ± 100 nM (mean ± SE) with a Hill coefficient of 1.38. Previously published data collected on native type 2 (Wt-T2) (Perez et al., 1997; Ramos-Franco et al., 1998a), native type 1 (Wt-T1) (Ramos-Franco et al., 1998a), and recombinant type 1 (R-T1) (Ramos-Franco et al., 1998b) $InsP_3R$ channels are presented by the broken lines. Note that the maximum P_o of both recombinant $InsP_3R$ channels (type 1 or type 2) appears to be less than

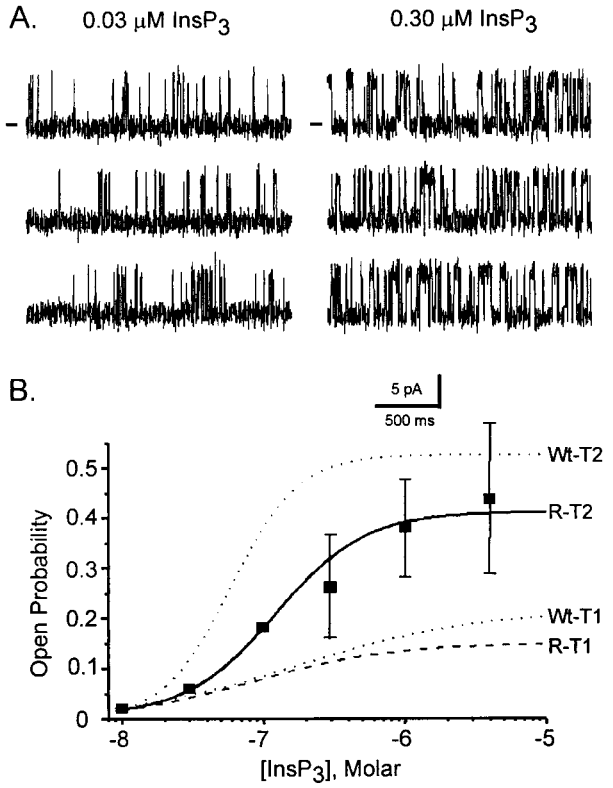

FIGURE 6 The $InsP_3$ sensitivity of single recombinant type 2 $InsP_3R$ channels. Recording solutions contained 220/20 mM $CsCH_3SO_3$ (*cis*/*trans*), 20 mM HEPES (pH 7.4), and 1 mM EGTA (250 nM free Ca^{2+}). The $InsP_3$ concentration on the cytoplasmic side of the channel was varied. Steady-state single-channel data were recorded at 0 mV. (*A*) Single-channel recordings at two different steady-state $InsP_3$ concentrations (0.03 and 0.30 μM). The zero-current level is marked. (*B*) Open probability plotted as a function of $InsP_3$ concentrations. Filled symbols represent means ($\pm$ SEM) of many measurements from several single $InsP_3R$ channels ($n = 4$). Recombinant type 2 $InsP_3R$ channel data (R-T2) are represented by the solid line and were best fit by a Hill equation with an apparent K_D of 122 $\pm$ 100 nM (mean $\pm$ SE) and a Hill coefficient of 1.38. Previously published recombinant (R-T1) and wild-type (Wt-T1) type 1 $InsP_3R$ channel data are represented as dashed lines (Ramos-Franco et al., 1998b). Previously published wild-type (Wt-T2) type 2 $InsP_3R$ channel data are also shown (Ramos-Franco et al., 1998a).

that of their native counterparts. Nevertheless, there was no significant difference between the maximum P_o values of the native and recombinant type 2 $InsP_3R$ channels (Table 2, *top*).

The Ca^{2+} sensitivity of the recombinant type 2 $InsP_3R$ channel was also defined. Sample single-channel recordings at three different free Ca^{2+} concentrations are presented in Fig. 7 *A*. These recordings were made at -20 mV; open events are shown as upward deflections. Like the $InsP_3$ sensitivity data presented above, the current carrier was a monovalent cation (Cs^+; 220/20 mM $CsCH_3SO_3$ gradient). The $InsP_3$ concentration on the *cis* side of the channel was 1 μM. The free Ca^{2+} concentration was adjusted by altering the Ca^{2+}-EGTA mixture and verified with a Ca^{2+} electrode. Channel activity increased when the free Ca^{2+} concentration was raised from 0.02 to 0.25 μM. A substantial level of spontaneous channel activity was evident, even at a relatively high free Ca^{2+} concentration (400 μM). Representative total amplitude histograms are presented to better illustrate the Ca^{2+}-dependent P_o changes (Fig. 7 *A, right*). The average open probability (P_o) of the channel is plotted as a function of Ca^{2+} concentration in Fig. 7 *B*. These data points (mean $\pm$ SE) represent recordings from seven different channels. Peak activation of the recombinant type 2 $InsP_3R$ channel (*solid line*, R-T2) occurred at the 250 nM Ca^{2+} mark. Previously published data collected on native type 2 (Wt-T2), native type 1 (Wt-T1), and recombinant type 1 (R-T1) $InsP_3R$ channels are represented by the broken lines (Ramos-Franco et al., 1998a,b). The Ca^{2+} sensitivities of the native and recombinant type 1 $InsP_3R$ channels were bell-shaped. The Ca^{2+} sensitivities of the native and recombinant type 2 $InsP_3R$ channels were more sigmoidal in nature, with substantial channel activity occurring at high Ca^{2+} concentrations. The absolute value of peak P_o was not statistically different between native and recombinant type 2 $InsP_3R$ channels (Table 2, *bottom*), and the overall shapes of their Ca^{2+} dependencies were remarkably similar.

DISCUSSION

This study reports the expression of the full-length type 2 $InsP_3R$ and demonstrates that the protein encoded forms functional ion channels with properties similar to those of the native type 2 receptor from ventricular cardiac myocytes. The type 2 $InsP_3R$, when transiently transfected into COS-1 cells, was expressed at high levels and was targeted to the endoplasmic reticulum. Immunoblot studies demonstrate that overexpression of the recombinant type 2 $InsP_3R$ in COS cells did not result in up-regulation of endogenous $InsP_3R$ expression. This is consistent with our earlier experience with the expression of recombinant type 1 $InsP_3R$ in COS-1 cells (Ramos-Franco et al., 1998b). Microsomal fractions isolated from $pInsP_3R$-T2 transfected COS-1 cells specifically bound [^{3}H]$InsP_3$ at significant levels when compared to that of control (SS DNA). Saturation and competition radioligand binding predicts an apparent affinity of the recombinant type 2 isoform of $\sim$17 nM. Comparison of the full-length type 1 and 2 expression products reveals that the type 2 exhibit an approximately three- to fourfold higher apparent affinity for $InsP_3$ than the type 1 isoform. These results are consistent with those reported for the two isoforms' ligand-binding regions (Südhof et al., 1991).

Immunocytochemical analysis of transfected COS-1 cells, using the amino- and carboxyl-terminal antibodies, revealed that the recombinant type 2 $InsP_3R$ was targeted to the same structures (ER) as the type 1 $InsP_3R$ (Takei et al., 1994; Ramos-Franco et al., 1998b; Galvan et al., 1999).

TABLE 2 P_O values at 1 μM IP_3

Type 2 $InsP_3R$	Mean P_O	Standard error	No. of determinations	Two-tailed p value
P_O at 1 μM IP_3 in the presence of ~250 nM free Ca^{2+}				
Native	0.524	0.058	6	$p > 0.05$ (0.21)*
Recombinant	0.380	0.097	4	
P_O at 1 μM IP_3 in the presence of ~1 μM free Ca^{2+}				
Native	0.720	0.025	6	$p > 0.05$ (0.055)*
Recombinant	0.452	0.113	7	

* Not significant.

Some enrichment was also noted in the perinuclear and trans-Golgi regions. Cotransfection of COS-1 cells with different type 1 and 2 receptor constructs confirmed that the targeting of the two isoforms was very similar.

Most cells contain one or more endogenous $InsP_3R$ channels, and the COS-1 cell is no exception (Newton et al., 1994). Thus it is important to address the possibility that the $InsP_3R$ examined here are not simply endogenous channels. The experimental strategy applied here was to use an existing cell line (COS-1) and simply overexpress the recombinant receptor to the extent that any endogenous receptor present represents an almost negligible fraction of the total $InsP_3R$ pool. This strategy has previously been applied by two independent groups in defining the function of recombinant type 1 $InsP_3R$ channels in planar lipid bilayers (Ramos-Franco et al., 1998b; Kaznacheyeva et al., 1998). Several pieces of experimental evidence support the veracity of this experimental approach. First, Western blots of type 2 $InsP_3R$ in control (SS-DNA transfected) and test (p$InsP_3R$-T2) revealed that very little endogenous receptor was present compared to recombinant receptor. These data, together with those of previous studies using antibodies specific for the three $InsP_3R$ homologs, reveal that overexpression of one receptor isoform does not result in substantial up-regulation of endogenous receptors. Second, immunofluorescence data illustrated that COS-1 cells transfected with the type 2 receptor exhibited intense signals with the antibodies directed against the type 2 receptor. Third, microsomes from COS-1 cells transfected with the type 2 receptor bound $InsP_3$ at levels significantly above those of control (i.e., endogenous) and had an apparent affinity for ligand consistent with that reported for the type 2 receptor (Südhof et al., 1991). Fourth, no detectable $InsP_3R$ channels were found when proteoliposomes prepared from SS DNA transfected or nontransfected COS-1 cells were fused into planar lipid bilayers (Table 1; Ramos-Franco et al., 1998b). In contrast, frequent and robust single-channel activity was observed when proteoliposomes prepared from p$InsP_3R$-T2 transfected cells were fused into planar bilayers. Fifth, the $InsP_3$ and Ca^{2+} sensitivities of single recombinant type 1 and type 2 $InsP_3R$ channels were different, reflecting those of their native counterparts, indicating that the single $InsP_3R$ channel attributes observed correspond with the identity of the transfected cDNA construct. All of these data support the idea that the recombinant $InsP_3$ receptors dramatically outnumbered endogenous receptors in the pInsPR-T2-transfected COS-1 cells. Thus it is reasonable to conclude that the single-channel properties defined here represent the properties of the recombinant type 2 channel proteins.

The unitary conductance and gating of the single recombinant type 2 $InsP_3R$ channel were similar to those reported for native type 2 $InsP_3R$ channels (Perez et al., 1997; Ramos-Franco et al., 1998a). It is noteworthy that there appears to be a tendency for some channels (~60%) to be more open at negative voltages (Fig. 5, *A* and *B*). However, a significant fraction of channels (~40%) did not show this tendency. This variability evident in our single-channel records probably explains the relatively large error associated with the P_o measurements reported on the Ca^{2+} and $InsP_3$ dependency data plots.

The experimental conditions used here for the recombinant type 2 channels were similar to those we applied previously to native type 2 channels (Ramos-Franco et al., 1998a). This is consistent with the overall goal of this work of comparing the function of recombinant and native channels. Despite the relatively high variability associated with the P_o measurements and the small (< 20 mV) differences in steady-state holding potential, recombinant type 2 channel function was not significantly different compared to the native receptor (Table 2).

SUMMARY

The $InsP_3R$ gene family has been shown to be a fundamental component of many intracellular calcium-signaling pathways. Members within this small gene family of intracellular Ca^{2+} release channels have been shown to have a high degree of structural and functional homology. Despite the overall high degree of similarity in sequence and permeation properties between receptor types, each isoform appears to be subject to heterologous regulation by $InsP_3$ and Ca^{2+}. The data here demonstrate the expression and single-channel function of the full-length recombinant type 2 $InsP_3$

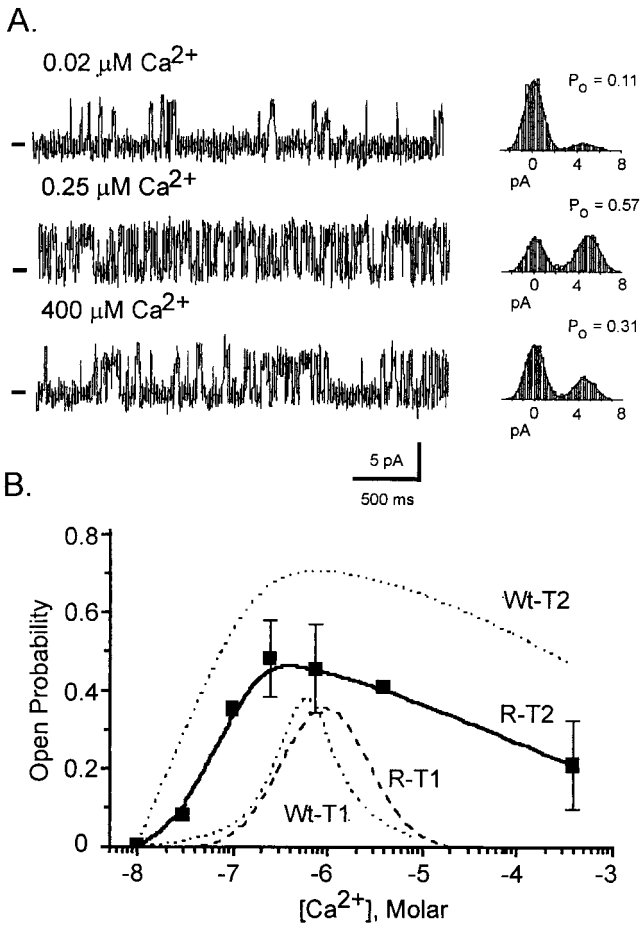

FIGURE 7 The Ca^{2+} sensitivity of single recombinant type 2 $InsP_3R$ channels. Recording solutions contained 220/20 mM $CsCH_3SO_3$ (*cis*/*trans*), 20 mM HEPES (pH 7.4), 1 mM EGTA, and 1 μM $InsP_3$. The free Ca^{2+} concentration on the cytoplasmic side of the channel was varied by changing the Ca-EGTA ratio. Steady-state single-channel data were recorded at −20 mV. (*A*) Single-channel recordings at three different steady-state Ca^{2+} concentrations (0.02, 0.25, and 400 μM). Open events are shown as upward deflections from the marked zero-current level. Corresponding total amplitude histograms collected at each Ca^{2+} concentration are shown at the right. Open probabilities calculated from fits of the histograms are indicated. (*B*) Open probability plotted as a function of free Ca^{2+} concentration. Filled symbols represent means (± SEM) of many measurements from several single $InsP_3R$ channels ($n = 7$). Recombinant type 2 $InsP_3R$ channel data (R-T2) are represented by the solid line and were fit by eye. Previously published recombinant (R-T1) and wild-type (Wt-T1) type 1 $InsP_3R$ channel data are represented as a dashed line (Ramos-Franco et al., 1998b). Previously published wild-type (Wt-T2) type 2 $InsP_3R$ channel data are also shown (Ramos-Franco et al., 1998a).

receptor. The functional attributes of the recombinant type 2 $InsP_3R$ at the single-channel level were very similar to its native counterpart. Thus this study establishes a tool that can be used to define the elements responsible for the unique regulatory properties of individual $InsP_3R$ receptor isoforms.

The authors extend many thanks to Dr. Thomas Südhof of the Howard Hughes Medical Institute, University of Texas Southwestern Medical Center at Dallas, for the kind gift of $InsP_3R$ cDNAs. We thank W. Jung and D. Galvan for preparation of the pEGFP-T1FL expression plasmid.

This work was supported by National Institutes of Health grants R29 MH 53367 (GM), RO1 HL58851 (GM), RO1 HL570832 (MF), and RO1 HL64210 (MF).

REFERENCES

Baudet, S. L., Hove-Madsen, and D. M. Bers. 1994. How to make and use calcium-specific mini- and microelectrodes. *Methods Cell Biol.* 40: 9–114.

Bezprozvanny, I., J. Watras, and B. E. Ehrlich. 1991. Bell-shaped calcium-response curves of Ins(1, 4, 5)P_3 and calcium gated channels from endoplasmic reticulum of cerebellum. *Nature.* 351:751–754.

Cameron, A. M., J. P. Steiner, A. J. Roskams, S. M. Ali, G. V. Ronnett, and S. H. Snyder. 1995. Calcineurin associated with the inositol 1,4,5-trisphosphate receptor-FKBP12 complex modulates Ca^{2+} flux. *Cell.* 83:463–472.

Galvan, D., E. Borrego-Diaz, P. J. Perez, and G. A. Mignery. 1999. Subunit oligomerization and topology of the inositol 1,4, 5-trisphosphate receptor. *J. Biol. Chem.* 274:29483–29492.

Gorman, C. 1985. High Efficiency Gene Transfer into Mammalian Cells. *In* DNA Cloning, Vol. II. D. M. Glover, editor. IRL Press, Oxford. 143–190.

Hagar, R. E., A. D. Burgstahler, M. H. Nathanson, and B. E. Ehrlich. 1998. Type III $InsP_3$ receptor channel stays open in the presence of increased calcium. *Nature.* 396:81–84.

Kaftan, E. J., B. E. Ehrlich, and J. Watras. 1997. Inositol 1,4, 5-trisphosphate ($InsP_3$) and calcium interact to increase the dynamic range of $InsP_3$ receptor-dependent calcium signaling. *J. Gen. Physiol.* 110:529–538.

Kaznacheyeva, E., V. D. Lupu, and I. Bezprozvanny. 1998. Single channel properties of inositol trisphosphate receptor heterologously expressed in HEK-293 cells. *J. Gen. Physiol.* 111:847–856.

Kiselyov, K., G. A. Mignery, M. X. Zhu, and S. Muallem. 1999. The N-terminal domain of the IP_3 receptor gates store-operated *hTrp3* channels. *Mol. Cell.* 4: 423–429.

Mak, D.-O. D., S. McBride, and J. K. Foskett. 1998. Inositol-1,4,5-trisphosphate activation of inositol trisphosphate receptor Ca^{2+} channel by ligand tuning of Ca^{2+} inhibition. *Proc. Natl. Acad. Sci. USA.* 95: 15821–15825.

Mak, D.-O. D., S. McBride, and J. K. Foskett. 2000. Effects of cytoplasmic calcium on calcium activation of recombinant rat type 3 inositol 1,4,5-trisphosphate receptor expressed in *Xenopus* oocytes. *Biophys. J.* 78: 313A.

Michikawa, T., J. Hirota, S. Kawano, M. Hiraoka, M. Yamada, T. Furuichi, and K. Mikoshiba. 1999. Calmodulin mediates calcium-dependent inactivation of the cerebellar type 1 inositol 1,4,5-trisphosphate receptor. *Neuron.* 23:799–808.

Mignery, G. A., P. A. Johnston, and T. C. Südhof. 1992. Mechanism of Ca^{2+} inhibition of inositol 1,4,5-trisphosphate ($InsP_3$) binding to the cerebellar $InsP_3$ receptor. *J. Biol. Chem.* 267:7450–7455.

Mignery, G. A., C. L. Newton, B. T. Archer III, and T. C. Südhof. 1990. Structure and expression of the rat inositol-1,4,5-trisphosphate receptor. *J. Biol. Chem.* 265:12679–12685.

Mignery, G. A., and T. C. Südhof. 1993. Molecular analysis of inositol 1,4,5-trisphosphate receptors. *Methods Neurosci.* 18:247–265.

Mignery, G. A., T. C. Südhof, K. Takei, and P. DeCamilli. 1989. Putative receptor for inositol 1,4,5-trisphosphate similar to ryanodine receptor. *Nature.* 342:192–195.

Miyakawa, T., A. Maeda, T. Yamazawa, K. Hirose, T. Kurosaki, and M. Iino. 1999. Encoding of Ca^{2+} signals by differential expression of IP_3 receptor subtypes. *EMBO J.* 18:1303–1308.

Newton, C. L., G. A. Mignery, and T. C. Südhof. 1994. Co-expression in vertebrate tissues and cell lines of multiple inositol 1,4,5-trisphosphate

($InsP_3$) receptors with distinct affinities for $InsP_3$. *J. Biol. Chem.* 269: 28613–28619.

Perez, P. J., J. Ramos-Franco, M. Fill, and G. A. Mignery. 1997. Identification and functional reconstitution of the type 2 $InsP_3$ receptor from ventricular cardiac myocytes. *J. Biol. Chem.*:272: 23961–23969.

Ramos-Franco, J., M. Fill, and G. A. Mignery 1998a. Isoform specific function of single inositol 1,4,5-trisphosphate receptor channels. *Biophys. J.* 75*:*834–839.

Ramos-Franco, J., M. Fill, and G. A. Mignery. 1998b. Single channel function of recombinant type 1 inositol 1,4,5-trisphosphate receptor ligand binding domain splice variants. *Biophys. J.* 75:2783–2793.

Sayers, L. G., A. Miyawaki, A. Muto, H. Takeshita, A. Yamamoto, T. Michikawa, T. Furuichi, and K. Mikoshiba. 1997. Intracellular targeting and homotetramer formation of a truncated inositol 1,4,5-trisphosphate receptor-green fluorescent protein chimera in *Xenopus laevis* oocytes: evidence for the involvement of the transmembrane spanning domain in endoplasmic reticulum targeting and homotetramer formation. *Biochem. J.* 323:273–280.

Südhof, T. C., C. L. Newton, B. T. Archer, Y. A. Ushkaryov, and G. A. Mignery. 1991. The structure of a novel $InsP_3$ receptor. *EMBO J.* 10:3199–3206.

Takei, K., G. A. Mignery, E. Mugnaini, T. C. Südhof, and P. De Camilli. 1994. Inositol 1,4,5-trisphosphate receptor causes formation of ER cisternal stacks in transfected fibroblasts and in cerebellar Purkinje cells. *Neuron.* 12:327–342.

Watras, J., I. Bezprozvanny, and B. E. Ehrlich. 1991. Inositol 1,4,5-trisphosphate-gated channels in cerebellum: presence of multiple conductances states. *J. Neurosci.* 11:3239–3245.

Watras, J., S. Syrbu, and B. E. Ehrlich. 1999. An endogenous inhibitor of $InsP_3$ binding isolated from cerebellar microsomes. *Biophys. J.* 76: A3375.